Biophysical Chemistry 167 (2012) 36–42

Contents lists available at SciVerse ScienceDirect

Biophysical Chemistry

journal homepage: http://www.elsevier.com/locate/biophyschem

Thermal denaturation of a blue-copper laccase: Formation of a compact denatured state with residual structure linked to pH changes in the region of histidine protonation

Citlali Toledo-Núñez [a], Javier I. López-Cruz [b], Andrés Hernández-Arana [a,*]

[a] Departamento de Química, Área de Biofisicoquímica, Universidad Autónoma Metropolitana-Iztapalapa, D.F. 09340, Mexico
[b] Departamento de Biotecnología, Universidad Autónoma Metropolitana-Iztapalapa, D.F. 09340, Mexico

HIGHLIGHTS

- The absolute heat capacity of a blue-copper laccase was determined from DSC scans.
- Above pH 7.5, the denatured laccase behaves as a fully solvated polypeptide chain.
- From pH 4.5 to 5.5, a compact denatured state with residual structure is formed.
- Stability of the compact state seems to be linked to protonation of His residues.

GRAPHICAL ABSTRACT

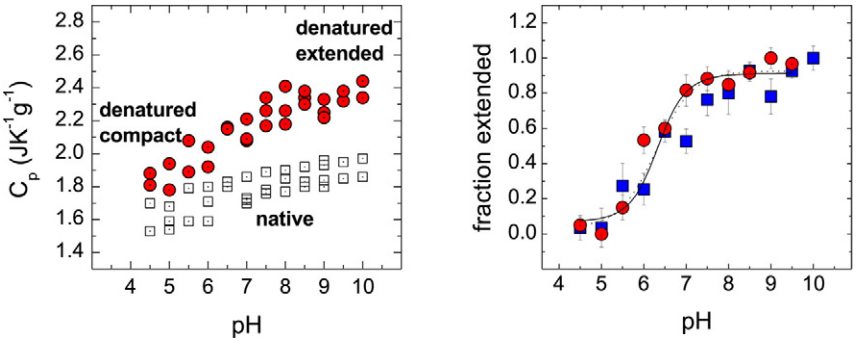

ARTICLE INFO

Article history:
Received 15 March 2012
Received in revised form 28 April 2012
Accepted 29 April 2012
Available online 5 May 2012

Keywords:
Blue-copper laccase
Thermal denaturation
Compact denatured state
Partial (absolute) heat capacity
Residual structure

ABSTRACT

The partial (absolute) heat capacity of a laccase enzyme from *Myceliophthora thermophila* (MtL) was determined from calorimetric scans in the 4.5–10.0 pH range. Above pH 7.5, the heat capacity of the thermally denatured state (C_p^D) of this blue-copper glycoprotein is consistent with that for an unfolded, fully solvated polypeptide chain, if its carbohydrate content is taken into account. Below pH 7.5, C_p^D decreases and eventually levels off within the 5.5–4.5 pH region, where a compact, partially solvated denatured state is formed. In the compact state, denatured MtL is an oligomer, and exhibits considerable native-like secondary structure and a perturbed environment of its copper atoms. Analysis of the pH dependence of C_p^D and the content of secondary structure gives results implying that His residues play an important role in the stability of the compact denatured state.

1. Introduction

In studies looking for the molecular basis of protein thermostability, it has been found that various structural factors seem to contribute to the resistance of proteins to heat denaturation, either when this process is reversible (thermodynamic stability) or irreversible (kinetic stability) [1–4]. Among these factors, those that lead to the persistence of residual structure in denatured states have received increased attention during the last decade [5–8].

In general, interactions tethering different regions of a protein molecule are thought to increase the stability of the native state, but they can also modulate the stability of the denatured state [6]. Specifically, the persistence of electrostatic interactions, and its relationship to the structural characteristics of denatured proteins

* Corresponding author. Tel.: +51 55 5804 4674; fax: +51 55 5804 4666.
E-mail address: aha@xanum.uam.mx (A. Hernández-Arana).

0301-4622/$ – see front matter © 2012 Elsevier B.V. All rights reserved.
doi:10.1016/j.bpc.2012.04.004

have been highlighted in several reports [5,6,9–11]. Histidine–metal binding may also be a source of conformational constraints that promote the formation of persistent nonrandom structure in denatured states [6]. In some glycoproteins, covalently linked sugar moieties are known to establish well-defined hydrogen bonds and hydrophobic interactions with the protein chain [12,13]. Possibly, glycan–protein interactions can also be responsible, at least in part, for the presence of residual structure in compact denatured states [14,15].

Because the presence of structured regions in the unfolded state is expected to reduce the surface area exposed to solvent, calorimetric measurements of the change in heat capacity upon unfolding (ΔC_p), which in turn is proportional to the increment in solvent-accessible surface area (ΔASA) [16,17], have been widely used to detect residual structure in thermally denatured proteins [6]. Nevertheless, to be certain that an atypically small ΔC_p value is indicative of residual structure in the denatured state of a protein, the partial or absolute heat capacity of the native (C_p^N) and denatured states (C_p^D) must both be determined [8].

In this work, we carried out a calorimetric study of the thermal denaturation of a copper-containing laccase glycoprotein from the thermophilic fungus *Myceliophthora thermophila* (henceforth abbreviated MtL). A highly sensitive scanning nanocalorimeter was used to determine C_p^N and C_p^D at different pH values. Between pH 5.5 and 7.5, C_p^D showed a notable increase that correlates with changes observed in the far-UV circular dichroism (CD) spectrum of the denatured laccase. These findings point out the presence of residual structure in denatured MtL around pH 4.0 to 5.5, inasmuch as only minor variation was found for C_p^N values and CD spectra within whole studied pH range. It should be noted that in a survey of the literature we have found a few reports of ΔC_p determinations for unfolding of glycoproteins, but in none of them absolute heat capacities seem to have been determined. In this regard, our C_p^N and C_p^D determinations for MtL should contribute to the knowledge of the thermal properties of complex conjugated proteins.

2. Materials and methods

2.1. Materials

The enzyme MtL was obtained from the company Novo Nordisk, in the form of a commercial preparation called Deni Lite IIs. 2′,2-azinobis(3-ethylbenzothiazoline-6-sulfonic acid) (ABTS), 2,6-dimethoxyphenol (DMP) were from Sigma (St. Louis, MO).

2.2. Extraction and purification of laccase

MtL was purified by several steps of centrifugation, ultrafiltration and anion-exchange chromatography, as previously described [18]. SDS-polyacrylamide gel electrophoresis (SDS page) was performed in order to check the purity of the preparation. The concentration of MtL was determined spectrophotometrically at 280 nm using a calculated extinction coefficient ($128.62\times10^3\ M^{-1}\ cm^{-1}$) based on the content of aromatic residues and disulfide bonds [19].

2.3. Mass spectroscopy

One microliter of laccase solution (3.8 mg mL^{-1} in 10 mM sodium phosphate buffer, pH 6.0) was mixed with five microliters of the matrix (either sinapinic acid or 2,5-dihydroxybenzoic acid) and analyzed in a Microflex matrix-assisted laser desorption ionization time-of-flight instrument (Bruker Daltonik GmbH, Leipzig, Germany) equipped with a 20-Hz nitrogen laser. Spectra were recorded in the positive linear mode for high mass range. Bovine serum albumin was used as standard.

2.4. Activity assays

Laccase activity was assayed at room temperature by measuring the rate of ABTS oxidation [20]. The reaction mixture contained 900 μL of 5 mM ABTS dissolved in 50 mM sodium phosphate buffer (pH 6.0) and 100 μL of appropriately diluted enzyme. ABTS oxidation was followed by the increase of absorbance at 420 nm ($\varepsilon_{420} = 36000\ M^{-1}\ cm^{-1}$). For determination of catalytic constants, ABTS solutions were prepared in the phosphate buffer (pH 6.0) at concentrations varying from 0.002 to 4.5 mM.

2.5. Circular dichroism

CD measurements were performed in a Jasco J-715 spectropolarimeter (Jasco Inc., Easton, MD) equipped with a PTC-348WI Peltier-type cell holder for temperature control. Far-UV spectra (250–190 nm) were recorded using MtL solutions (15–300 μg mL^{-1}) that were equilibrated against the appropriate buffer (10 mM sodium citrate, 20 mM sodium phosphate or 20 mM sodium borate, depending on the desired pH value), and placed in 1.00-, 0.20-, or 0.05-cm cells, depending on the protein concentration. In the near-UV region (320–250 nm), laccase solutions of ca. 1.0 mg mL^{-1} and a 1.00-cm cell were employed.

Native MtL spectra were obtained at 25 °C from freshly prepared samples. These samples were heated up to 92 °C (maximal temperature allowed by our experimental setup) and let stand at this temperature until no further changes in ellipticity were noticed; spectra for denatured MtL were then registered. Afterward, samples were cooled down to 25 °C and their spectra again recorded to check on the reversibility of thermal denaturation. Temperature-induced denaturation transitions were monitored by recording the ellipticity (either at 202 or 284 nm) while the sample temperature was increased at a constant rate. Protein solutions ca. 15 μg mL^{-1} (for the far-UV) and 1.0 mg mL^{-1} (for the near-UV), and a 1.00-cm cell were used. The temperature inside the cell was measured with the external probe of the cell holder. Our experimental setup allowed for constant heating-rate up to 89 °C. Unfolding transitions of hen-egg white lysozyme were used as an external standard to calibrate the temperature readings from the CD and DSC instruments (see Section 2.7) against each other.

2.6. UV–vis absorption

Measurements of light absorption were carried out in a G1103A UV/Visible Spectrophotometer (Agilent Technologies). Buffers employed were the same as those used for DC and DSC experiments. Absorption spectra of laccase solutions (ca. 1.0 mg mL^{-1}) were registered from 800 to 270 nm, in a 1.00-cm quartz cell. Changes in light absorption (600 nm) with time were measured as described above for DC experiments.

2.7. Differential scanning calorimetry

DSC was performed on a nano differential scanning calorimeter (Nano DSC 6300; TA Instruments-Waters LLC) equipped with capillary cells of 0.300 mL. Protein concentrations used in the DSC studies varied between 2.0 and 4.0 mg mL^{-1}. Protein samples were extensively dialyzed against the desired reference buffer. All solutions were properly degassed and carefully loaded into the cells to avoid bubble formation. Both cells were pressurized to nearly 3.0 atm and heated from 5 to 120 °C at constant rate (typically, 0.5 °C min^{-1}). Six to seven reference scans with buffer-filled cells preceded each sample run to achieve near perfect baseline repeatability; buffer collected from the final dialysis of a protein sample was used for buffer–buffer scans. In most cases, samples were scanned twice to assess the reversibility of MtL denaturation and to determine the

heat capacity of the denatured protein. The software package provided by the manufacturer was used for data analysis, including baseline subtraction and determination of denaturation enthalpy. Absolute heat capacities were calculated by means of the following equation [8,21]:

$$C_p = \left(C_{p,p} - C_{p,b}\right) / \left(v_{cel} \cdot c\right) + C_{p,b}{}^0 \left(V_p{}^0 / V_b{}^0\right) \quad (1)$$

where $C_{p,p}$ and $C_{p,b}$ refer to the heat capacity (J/K) measured with the protein and buffer solutions, respectively; v_{cel} is the volume of the calorimetric cell (in mL) and c is the protein concentration (g/mL) used for the experiment. $C^0_{p,b}$ is the specific heat capacity of the buffer solution; V^0_p and V^0_b are the partial specific volumes of the protein and solvent, respectively. The partial molar volume of MtL was taken as that of its 620 constituent amino acid residues (computed from the partial molar volumes of amino side chains and of the peptide unit [22]) plus an estimated volume value due to its carbohydrate content (9.8%, as deduced from mass spectroscopy; see Section 3.1); because all the sugar moieties present in MtL appear to be derived from hexoses [20], we used data available in the literature [23] for some hexoses (i.e., galactose, glucose, and fructose) and their disaccharides (i.e., sucrose, lactose, and maltose) to estimate the average partial molar volume of a hexosyl residue in the laccase. Reported heat capacity values are the average of individual values from at least three different DSC runs carried out in solutions of the same pH but with different protein concentration.

2.8. Dynamic light scattering

DLS measurements were performed on a Zetasizer Nano S dynamic light-scattering instrument (Malvern Instruments, Worcestershire, UK) as described in [24]. Buffer and MtL (0.9 mg mL^{-1}) solutions were filtered down to 0.22 μm immediately before use, and care was taken to reduce contamination of samples by dust. Solutions were placed in a quartz cell (50 μL) and equilibrated to 25 °C; at least 15 measurements of six seconds each were collected for each sample. Zetasizer 6.2 software was used to calculate size distributions.

3. Results

3.1. Structural properties of native MtL

An alignment of amino acid sequences including MtL and two other fungal laccases, whose three-dimensional structures are known, revealed that the sequence of MtL is 69 and 75% identical with those of the enzymes from *Thiolavia arenaria* and *Melanocarpus albomyces*, respectively. High similarity was specially observed in sequence regions with β-strand conformation; positions of histidine residues that act as ligands of the four copper atoms essential for enzymatic activity are also conserved in the sequence of MtL. It is likely, therefore, that MtL shares the general folding pattern of blue-copper fungal laccases [25] whose molecular structures show three well-defined domains. In accord with this, the far-UV CD spectrum of native MtL (Fig. 1A) displayed characteristics typical of all-β proteins. Similarly, a light-absorption band ca. 600 nm (results not shown) characterizes this enzyme as a blue-copper laccase [25,26]. With ABTS as substrate, our purified MtL sample displayed catalytic constants ($K_M = 51$ μM; $k_{cat} = 3.5 \times 10^4$ s^{-1}) comparable to those for other fungal laccases [27]. The molecular mass of purified MtL, as determined by MALDI-TOF mass spectrometry (Fig. S1, Supplementary data) was 75,600 Da. By subtracting the mass of the 620 amino acid residues comprising the polypeptide chain of the enzyme and of four copper atoms, we estimate that the carbohydrate content of MtL is 9.8%.

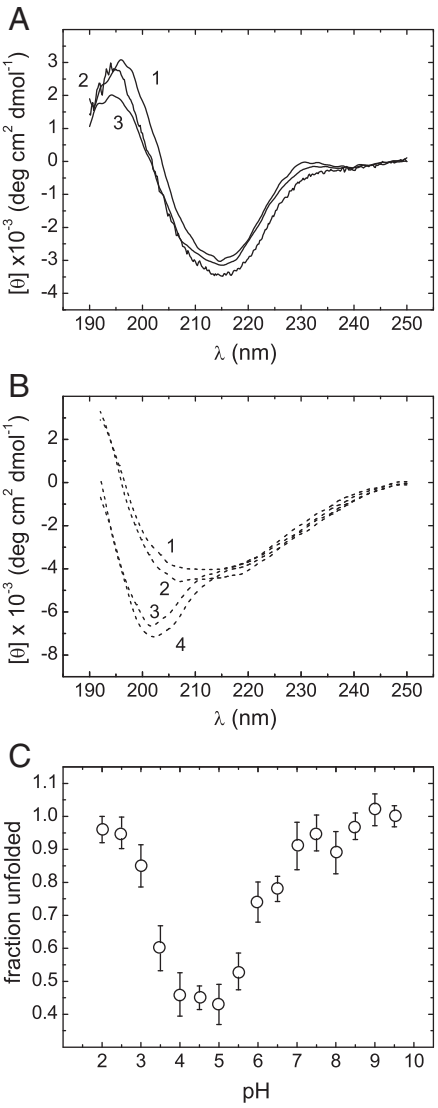

Fig. 1. CD spectra of native (A) and thermally denatured (B) MtL. Spectra in panel A were registered at 25.0 °C using fresh laccase solutions ca. 0.1 mg mL^{-1}, in a 0.100-cm cell, at different pH values: curve 1, pH 4.5; curve 2, pH 9.0; curve 3, pH 2.5. Spectra for denatured MtL (B) were obtained at 92 °C from laccase samples that had been denatured in DSC experiments and then diluted to approximately 0.10 mg mL^{-1}; curves 1 to 4 refer to pH values of 4.5, 5.5, 2.5, and 9.0, respectively. Panel C shows the pH dependence of the fraction of completely unfolded protein, calculated from experimental spectra of denatured MtL as indicated in Section 3.4.1.

3.2. Thermal scans of MtL

As monitored by DSC, the thermal denaturation of MtL (pH 6.0) exhibits a complex profile (Fig. 2) comprising several individual transitions, which probably are due to the multidomain structure of this enzyme, and with low C_p magnitude (cf. the calorimetric trace for hen-egg white lysozyme which is also shown in Fig. 2 as curve 4). In rescans of thermally denatured MtL monotonically increasing curves were observed, indicating that the process is irreversible (see curve 2 in Fig. 2). Neither the thermogram shape nor the irreversible behavior of MtL denaturation was affected by the presence of 0.125 mM Cu^{2+} ions in the solution. Increasing of scan rate resulted in shifts of calorimetric signals towards higher temperature (cf. curves 1 and 3 in Fig. 2), as expected for thermal transitions under kinetic control [4]. It should be stressed, however, that thermal scans are not complicated by exothermic effects at high temperatures, effects that appear in several proteins that denature irreversibly. Furthermore, the coincidence of C_p values in the high-temperature

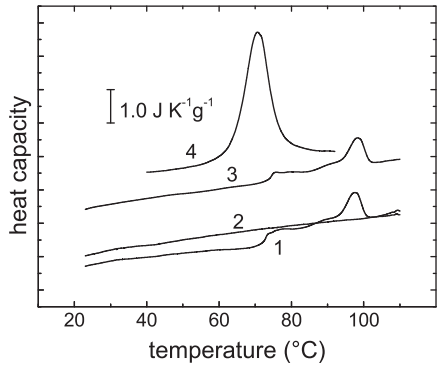

Fig. 2. DSC profiles of MtL solutions (ca. 2.0 mg mL^{-1}) at pH 6.0. Curve 1: native protein, 0.5 °C min^{-1}; curve 2: second scan of the experiment shown in curve 1; curve 3: native protein, 1.0 °C min^{-1}. For the sake of comparison, the C_p tracing for hen-egg white lysozyme (pH 3.0) is also shown (curve 4).

end of the first scan and the rescan suggests that this latter can be used to determine the heat capacity of denatured MtL (C_p^D).

Thermal scans of MtL were also followed by monitoring the CD signal (either at 202 or 284 nm) as the temperature increased at 0.5 °C min^{-1}. Due to technical limitations, denaturation profiles were restricted to temperatures below 90 °C. However, these scans were useful to observe part of the conformational changes that take place upon denaturation. As shown in Fig. S2 (Supplementary data), the onset of changes in secondary structure nearly coincides with the initial, sharp increase in C_p observed in DSC scans (cf. Fig. 2, curve 1), whereas the loss of tertiary structure seems to begin at slightly lower temperature.

Further DSC experiments in different pH conditions were carried out mainly at 0.5 °C min^{-1}, because sharper, better resolved signals were obtained with this heating rate. Owing to the low magnitude of endothermic peaks, protein concentration was kept above 2.0 mg mL^{-1} in order to obtain more accurate determinations of heat capacities and enthalpy changes. Fig. 3 gives an overview of the effect of pH on the appearance of MtL thermograms. As can be seen, the number and relative magnitudes of individual transitions observed in thermal scans are conserved within the 4.5–9.5 pH range; at pH values lower than 4.0 clear exothermic distortions were observed at middle and high temperatures. Likely, aggregation of denatured laccase, as well as of some partially denatured intermediates, takes place at pH near the isoelectric point of the enzyme (pI–3.8). Indeed, evident sample aggregation was observed after a first scan was run in acid media.

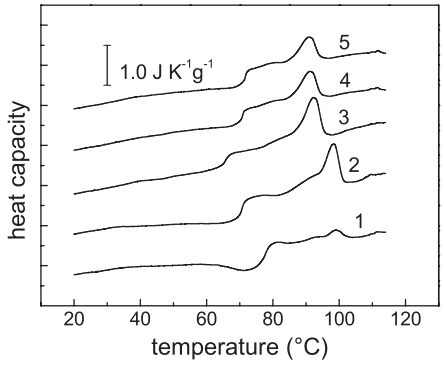

Fig. 3. DSC profiles of MtL recorded at different pH values. Curve 1, pH 4.5; curve 2, pH 6.0; curve 3, pH 7.5; curve 4, pH 8.5; curve 5, pH 9.5. The scan rate was 0.5 °C min^{-1} in all cases.

3.3. Absolute specific heat capacities for native (C_p^N) and denatured (C_p^D) MtL

Values of C_p^N and C_p^D, determined as the average of individual thermograms according to Eq. (1) (Materials and methods), are plotted as a function of pH in Fig. 4. It can be observed that C_p^D follows a sigmoidal trend, which is more readily seen at 106.0 °C, with a significant increase between pH 5.5 and 7.5. To compare C_p^D values for MtL at 25.0 °C with that expected for a fully solvated unfolded state, the contribution of peptide groups and amino acid side chains was calculated according to either Makhatadze and Privalov [28] or Hackel et al. [29]. To the heat capacity for the protein we added a part corresponding to glycan moieties, which was estimated from the carbohydrate content of MtL and the average of heat capacities for different mono- and disaccharides at 25.0 °C [30]. As seen in Fig. 4, at pH values above 7.5 our experimental determinations of C_p^D lie between the two estimated values. Contrasting with the behavior of C_p^D, the heat capacity of native MtL showed a slight, linear increase when pH was raised from 4.0 to 10.0. Within this range, C_p^N averages out to 1.79 ± 0.14 J K^{-1} g^{-1}. For 12 native, non-conjugated proteins, the average heat capacity amounts to 1.46 ± 0.07 J K^{-1} g^{-1} [31]. By adding the weighted contribution from glycan chains, we obtain for native MtL an expected C_p^N (1.50 J K^{-1} g^{-1}) that is about 16% smaller than the experimental value. It must be recognized, however, that the comparison between experimental and calculated C_p values should be taken with caution, inasmuch as the contribution from the carbohydrate moieties to the heat capacity represents only a rough approximation.

3.4. Physical properties of denatured MtL

3.4.1. Circular dichroism spectra

CD spectra for thermally denatured MtL were recorded at 92 °C using laccase samples that had been previously denatured in the nanocalorimeter, and then diluted to an appropriate concentration (ca. 0.10 mg mL^{-1}). In a second approach, spectra for heat-denatured MtL were obtained from native samples of low protein concentration (from 0.015 to 0.40 mg mL^{-1}) that were heated up to 92 °C and let stand at this temperature until no further changes in ellipticity were noticed. Within experimental error, the far-UV CD spectrum of denatured MtL was insensitive to the concentration of protein with which thermal denaturation was studied. In all cases, spectral changes observed upon denaturation at high temperature were not reversed after cooling of laccase samples to 25 °C.

Fig. 1B shows CD spectra representative of the effect of pH on the secondary conformation of denatured MtL. In acid or alkaline solutions, spectra acquire a particular shape and magnitude that is

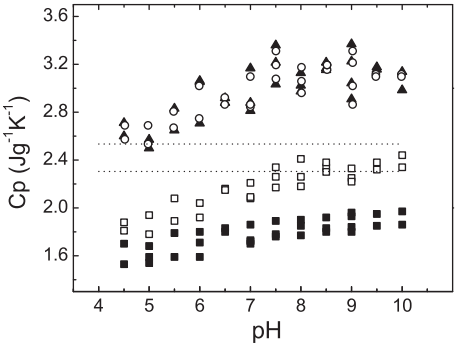

Fig. 4. Effect of pH on the partial (absolute) specific heat capacity of native and denatured MtL. Data corresponding to the native and denatured laccase, at 25 °C, are shown as filled and empty squares, respectively. Values of heat capacity for the denatured protein were also determined at 106 °C from the first scan of fresh samples (circles) and from the second scan of previously denatured samples (triangles).

characteristic of thermally unfolded proteins: a negative band of approximately 10×10^3 deg cm^2 dmol^{-1}, centered at 200–203 nm, and a negative shoulder with magnitude around 5×10^3 deg cm^2 dmol^{-1}. This type of CD spectrum is displayed by several small and medium-size proteins such as hen-egg lysozyme, ribonuclease A, cytochrome C, staphylococcal nuclease, cysteine proteases, etc., when unfolded at high temperature and in the absence of denaturants [32,33]. Otherwise, in the 4.0–5.5 pH range, spectra of denatured MtL resemble that of the native laccase (cf. Fig. 1A). To disclose the unfolded vs. native-like character present in denatured MtL at different pH values, its CD spectra were analyzed as a linear combination of two spectral types, namely, those for the native laccase and for the denatured form at high pH (this latter as representative of a typical thermally unfolded polypeptide chain). Results from this analysis (Fig. 1C) point out that the unfolded character accounts for only about 50% between pH 4.0 and pH 5.5, whereas its contribution increases to approximately 100% at extremes of pH. Noteworthily, increasing of the unfolded character with pH resembles the increase of C_p^D from pH 5.5 to 7.5 (Fig. 4). On the other hand, near-UV CD spectra (not shown) indicate an absence of tertiary structure in denatured MtL, regardless of the pH of the protein solution.

3.4.2. Vis–UV absorption spectra

MtL samples that had been denatured in DSC runs were also used to register Vis–UV absorption spectra. Fig. S3 (Supplementary data) shows difference spectra (i.e., denatured minus native MtL) corresponding to pH 5.5 and 9.0. Difference-absorption bands observed around 600 and 320 nm can be attributed to alterations in the environment of Cu^{2+} ions [26,34]; their signs and wavelength positions are consistent with changes in absorption observed upon thermal denaturation of other two fungal laccases [26]. On the other hand, the band centered ca. 289 nm probably reflects perturbation of tryptophan residues [35]. Overall, the larger magnitude of difference bands observed at pH 9.0 suggests that, upon denaturation, larger perturbations in the environment of Cu^{2+} ions and aromatic side-chains take place at high pH.

3.4.3. Aggregation state of denatured MtL

The size distributions, expressed as percent of volume occupied by particles of a given size, of denatured MtL at pH 5.5 and 9.0 are shown in Fig. S4 (Supplementary data); for the sake of comparison, the size distribution for the native laccase is also shown in this figure; it is seen there that at pH 9.0 denatured MtL increases only slightly in size with respect to the native protein; for spherical particles those sizes correspond to molecular masses of approximately 95 kDa (denatured) and 80.5 kDa (native). In contrast, at pH 6.0 denatured MtL shows a distribution centered at a size about twice that of the native species, indicating the formation of an oligomeric state comprising five or six molecules of MtL. It should be mentioned that, in all the distributions measured, aggregates of very large size were detected but they accounted for less than 2.0% of the total mass.

3.5. Enthalpy of denaturation

The enthalpy change associated to MtL denaturation (ΔH_d) was determined by integration of heat capacity traces, after subtraction of polynomial baselines constructed using the instrument software package. ΔH_d was found to be rather insensitive to pH changes, its value varying less than 40% within the studied pH interval (results not shown); a maximum value of approximately 13 J g^{-1}, which is reached near pH 6.0, represents about 50% of the specific unfolding enthalpy for non-conjugated proteins at 60 °C [16].

4. Discussion

4.1. Compact and extended forms of denatured MtL

Determinations of absolute (i.e., partial specific) heat capacities of *M. thermophila* laccase (MtL) indicate that, above pH 7.5, the thermally denatured state of this copper glycoprotein has a heat capacity, C_p^D, that agrees well with the value expected for an unfolded, fully solvated polypeptide chain (Fig. 4). However, the small value of C_p^D below pH 6.0 suggests that the denatured protein is only partially solvated at low pH; that is, a transition from a compact to an extended state (hereafter referred to as C and E states, respectively) of denatured MtL occurs in the 5.5–7.5 pH interval (Fig. 4). From the data in Fig. 4 we have computed denaturation ΔC_p values at high (ΔC_p^{E-N}) and low (ΔC_p^{C-N}) pH, obtaining average values of 0.45 and 0.27 Jg^{-1} K^{-1}, respectively. On account of the direct correlation between ΔC_p and ΔASA [16,17], the above values give a ΔASA for the N→C transition which is about 60% of the ΔASA for the N→E transition. In this regard, DLS measurements clearly show that at least part of the reduced solvent-accessible surface area in the C state is due to its oligomeric structure, which is comprised by five or six denatured monomers of the protein.

Other aspect that differentiates states C and E is the presence in the former of a large amount of native-like secondary structure, as detected by CD. This residual structure remains stable when protein concentration is decreased 26-fold, suggesting that this characteristic is independent of the oligomeric structure of state C and may, therefore, be another cause of the small ΔASA observed for the N→C denaturation transition.

The pH-induced change between states C and E is shown in Fig. 5, where the data from calorimetric and CD experiments are represented as the fraction of E state to display both data sets on the same ground. Data in Fig. 5 can be analyzed by taking into account the number of protons bound to states C (ν^C) and E (ν^E) and the well-known equation [36]:

$$d\ln K_{eq}/dpH = -2.303\left(\nu^E - \nu^C\right) \quad (2)$$

in which K_{eq} is the equilibrium constant for the transition from C to E. To express ν^C and ν^E as explicit functions of pH, we used the simplifying assumption that the ionizable side chains involved in the C to E transformation behave as independently titratable sites, each characterized by an acid dissociation constant, K_a. Then, the

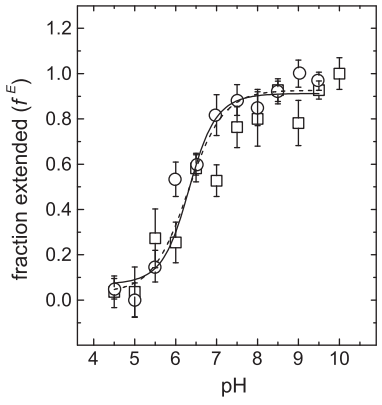

Fig. 5. Effect of pH on the interconversion of the compact and extended states of denatured MtL. The fraction of expanded state, f^E, was computed from heat capacity data (squares) and CD spectra (circles) of denatured MtL. Continuous lines are results from a fit of Eqs. (4) and (5) to f^E values: dashed line, fitting with $n=1$; solid line, fitting with $n=2$ (see Section 4.1). The fitting procedure gave pK values for the protonable sites relevant for the transformation of the compact into the extended state (Table 1).

protonation function for each site takes the simple form $\nu = a_H/(a_H + K_a)$, where a_H is the activity of protons in solution ($pH = -\log a_H$). If n sites have the same dissociation constant, the above expression becomes $\nu = n\ [a_H/(a_H + K_a)]$. It can be shown that by using this last expression for both ν^C and ν^E (with acid dissociation constants K_a^C and K_a^E, respectively) we can rewrite Eq. (2) as

$$d\ln K_{eq} = \sum n\left[da_H/\left(a_H + K_a{}^E\right) - da_H/\left(a_H + K_a{}^C\right)\right] \quad (3)$$

where use was made of the relationships $pH = -(1/2.303)\ln a_H$ and $dpH = -(1/2.303)\cdot(da_H/a_H)$. By performing integration, from a lower limit at which $a_H = 0$, we obtain:

$$\ln K_{eq} = \ln K_0 + n\cdot\ln\left[\left(K_a{}^C/K_a{}^E\right)\cdot\left(a_H + K_a{}^E\right)/\left(a_H + K_a{}^C\right)\right] \quad (4)$$

where K_0 is the value of K_{eq} in the limit $a_H = 0$. Eq. (4) is then used to compute the fraction of molecules in state E according to Eq. (5).

$$f^E = K_{eq}/\left(1 + K_{eq}\right). \quad (5)$$

Fitting of Eqs. (4) and (5) (with either $n = 1$ or $n = 2$) to f^E data resulted in curves of similar goodness of fit (dashed and solid lines in Fig. 5). However, results obtained under the assumption of two protonable sites (i.e., $n = 2$) gave more meaningful pK values for the sites involved and its associated errors (Table 1). Specifically, for the extended state of denatured MtL the value of pK^E is close to that for a histidine side chain in an unfolded protein [37]. In contrast, the value of pK^C is about one unit higher, suggesting that in the C state the putative histidines protonate more easily. These findings can be explained if one recalls that in laccase enzymes the electronegativity of His residues participating in copper binding is frequently enhanced by nearby Asp residues. Because the environment of Cu^{2+} ions is perturbed upon thermal denaturation of MtL, as difference UV–visible spectra indicate, some of the His–Cu^{2+} bonds are probably weakened or even broken in the denatured protein (for other laccases it has been reported that one Cu^{2+} ion is completely removed from the protein at 70 °C [26]). Breaking up of the His–Cu^{2+} bond would allow imidazole groups to easily protonate in a compact denatured state in which Asp side chains remain relatively close to His residues. In the denatured E state, however, the His and Asp residues will move away from each other, because they occupy distant positions in the polypeptide sequence, and the pK value of the imidazol group is expected to be rather typical, as mentioned above.

4.2. Enthalpy of denaturation

Regarding the enthalpy of denaturation for MtL, it is remarkable its small variation with pH, which points out that there is only a minor difference in enthalpy between states C and D. Thus, despite having residual secondary structure and low heat capacity, the compact denatured state seems similar to the extended unfolded state in enthalpy and in the lacking of tertiary structure. Overall, the characteristics of C state are remindful of molten-globule-like structures that have been found in compact denatured forms of proteins such as α-lactalbumin, staphylococcal nuclease, and apomyoglobin [38,39]. In relation to native states, these "molten globules" are conceived as structures that are expanded but with no many water molecules included in them. It is thought, thus, that their temperature-induced unfolding occurs with a barely noticeable enthalpy change owing to compensation of the heat absorption required to disrupt residual interactions between protein groups (i.e., hydrogen bonds remaining in elements of secondary structure, and some weakened van der Waals contacts) by the heat-evolving effect from hydration of these groups; extensive hydration, however, results in a large increase in the molecule's heat capacity [38,39].

Another salient observation concerning the specific denaturation enthalpy of MtL is that it amounts to only half the average value found in other proteins. Although small denaturation enthalpies have been reported for a few glycoproteins, such a result is by no means the norm for this type of macromolecules [40]. In the particular case of MtL, it is important to note the sigmoid-like, sharp increase in heat capacity observed in the low-temperature region of thermal DSC scans (Fig. 3); this transition, which was overlooked in a previous work from our laboratory [18] that was carried out with a less sensitive instrument, is accompanied with changes in secondary and tertiary structure (Fig. S2). Similar C_p transitions have been observed before in the low-temperature region of DSC scans of a calcium-binding protein [41], as well as in the unfolding of a "molten globule" intermediate of apomyoglobin [39]. As Griko and Privalov have noted [38,39], a thermal transition that proceeds with a change in heat capacity but with negligible heat absorption, such as that of apomyoglobin at pH 4.0, is better described as a second-order phase transition; theoretically, transitions of this kind are predicted for the unfolding of molten globules due to the absence of specific tertiary interactions in their structures [38,39,42]. Perhaps a loosely packed region in the structure of native laccase accounts for both the low-temperature sigmoid C_p transition observed upon thermal denaturation and the small value of the global denaturation enthalpy. Inasmuch as looser packing has been observed at domain interfaces of large proteins [43], an extensive interdomain region in MtL would likely appear as responsible for the rather peculiar thermal behavior of this protein. However, further studies are required to establish whether this is so or not.

Supplementary data to this article can be found online at http://dx.doi.org/10.1016/j.bpc.2012.04.004.

Table 1
pK values for the protonable sites involved in the transition from the compact to the extended forms of denatured MtL.

n [a]	pK^C	pK^E
1	7.40 (0.15)	4.90 (0.50)
2	6.80 (0.10)	5.80 (0.13)

pK values in the compact (pK^C) and extended (pK^E) denatured states of MtL were obtained from fitting of Eqs. (4) and (5) to the data in Fig. 5. Standard errors are shown in parenthesis.

[a] n is the number of independent protonable sites with identical pK value that were included in the fitting procedure.

Acknowledgments

We are grateful to J.M. Sanchez-Ruiz (Facultad de Ciencias, Departamento de Química Física, Universidad de Granada, Spain) for many helpful suggestions and comments on the development of this work, and for allowing C.T.N to carry out some research activities at his laboratory. We would like to thank Dr. Adela Rodríguez-Romero and Dr. Alejandra Hernández-Santoyo (Instituto de Química, UNAM, México) for their help in performing mass spectroscopy and dynamic light scattering experiments.

This work was funded in part by CONACYT, México (SEP-CONACYT 2007–80457).

References

[1] A. Razvi, J.M. Scholtz, Lessons in stability from thermophilic proteins, Protein Science 15 (2006) 1569–1578.
[2] K.A. Luke, C.L. Higgins, P. Wittung-Stafshede, Thermodynamic stability and folding of proteins from hyperthermophilic organisms, The FEBS Journal 274 (2007) 4023–4033.
[3] S. Kumar, R. Nussinov, How do thermophilic proteins deal with heat? CMLS Cellular and Molecular Life Sciences 58 (2001) 1216–1233.
[4] J.M. Sanchez-Ruiz, Protein kinetic stability, Biophysical Chemistry 148 (2010) 1–15.

[5] C.N. Pace, B.M.P. Huyghues-Despointes, H. Fu, K. Takano, J.M. Scholtz, G.R. Grimsley, Urea denatured state ensembles contain extensive secondary structure that is increased in hydrophobic proteins, Protein Science 19 (2010) 929–943.
[6] B.E. Bowler, Thermodynamics of protein denatured states, Molecular BioSystems 3 (2007) 88–99.
[7] Y. Li, F. Picart, D.P. Raleigh, Direct characterization of the folded, unfolded, and urea-denatured states of the C-terminal domain of the ribosomal protein L9, Journal of Molecular Biology 349 (2005) 839–846.
[8] M. Guzman-Casado, A. Parody-Morreale, S. Robic, S. Marqusee, J.M. Sanchez-Ruiz, Energetic evidence for formation of a pH-dependent hydrophobic cluster in the denatured state of *Thermus thermophilus* ribonuclease H, Journal of Molecular Biology 329 (2003) 731–743.
[9] N.C. Fitzkee, B. García-Moreno E, Electrostatic effects in unfolded staphylococcal nuclease, Protein Science 17 (2008) 216–227.
[10] J.H. Cho, D.P. Raleigh, Electrostatic interactions in the denatured state and in the transition state for protein folding: effects of denatured state interactions on the analysis of transition state structure, Journal of Molecular Biology 359 (2006) 1437–1446.
[11] C.F. Lee, M.D. Allen, M. Bycroft, K.B. Wong, Electrostatic interactions contribute to reduced heat capacity change of unfolding in a thermophilic ribosomal protein L30e, Journal of Molecular Biology 348 (2005) 419–431.
[12] S. Sinha, A. Surolia, Attributes of glycosylation in the establishment of the unfolding pathway of soybean agglutinin, Biophysical Journal 92 (2007) 208–216.
[13] N. Mitra, S. Sinha, T.N.C. Ramya, A. Surolia, *N*-linked oligosaccharides as outfitters for glycoprotein folding, form and function, Trends in Biochemical Sciences 31 (2006) 156–163.
[14] A. Sarkar, P.L. Wintrode, Effects of glycosylation on the stability and flexibility of a metastable protein: the human serpin α_1-antitrypsin, International Journal of Mass Spectrometry 302 (2011) 69–75.
[15] J. de Groot, H.A. Kosters, H.H.J. de Jongh, Deglycosylation of ovalbumin prohibits formation of a heat-stable conformer, Biotechnology and Bioengineering 97 (2007) 735–741.
[16] A.D. Robertson, K.P. Murphy, Protein structure and the energetics of protein stability, Chemistry Review 97 (1997) 1251–1267.
[17] J.K. Myers, C.N. Pace, J.M. Scholtz, Denaturant *m* values and heat capacity changes: relation to changes in accessible surface areas of protein unfolding, Protein Science 4 (1995) 2138–2148.
[18] J.I. López-Cruz, G. Viniegra-González, A. Hernández-Arana, Thermostability of native and pegylated *Myceliophthora thermophila* laccase in aqueous and mixed solvents, Bioconjugate Chemistry 17 (2006) 1093–1098.
[19] C.N. Pace, F. Vajdos, L. Fee, G. Grimsley, T. Gray, How to measure and predict the molar absorption coefficient of a protein, Protein Science 4 (1995) 2411–2423.
[20] R.M. Berka, P. Schneider, E.J. Golightly, S.H. Brown, M. Madden, K.M. Brown, T. Halkier, K. Mondorf, F. Xu, Characterization of the gene encoding an extracellular laccase of *Myceliophthora thermophila* and analysis of the recombinant enzyme expressed in *Aspergillus oryzae*, Applied and Environmental Microbiology 63 (1997) 3151–3157.
[21] E. Freire, in: B.A. Shirley (Ed.), Protein stability and folding: theory and practice, Methods in molecular biology, vol. 40, Humana Press, Totowa, 1995, p. 191.
[22] G.I. Makhatadze, V.N. Medvedkin, P.L. Privalov, Partial molar volumes of polypeptides and their constituent groups in aqueous solution over a broad temperature range, Biopolymers 30 (1990) 1001–1010.
[23] P.C. Dey, M.A. Motin, T.K. Biswas, E.M. Huque, Apparent molar volume and viscosity studies on some carbohydrates in solutions, Monatshefte für Chemie 134 (2003) 797–809.
[24] A. Hernández-Santoyo, A. Landa, E. González-Mondragón, M. Pedraza-Escalona, R. Parra-Unda, A. Rodríguez-Romero, Crystal structure of Cu/Zn superoxide dismutase from *Taenia solium* reveals metal-mediated self-assembly, The FEBS Journal 278 (2011) 3308–3318.
[25] U.N. Dwivedi, P. Singh, V.P. Pandey, A. Kumar, Structure–function relationship among bacterial, fungal and plant laccases, Journal of Molecular Catalysis B: Enzymatic 68 (2011) 117–128.
[26] O.V. Koroleva, E.V. Stepanova, V.I. Binukov, V.P. Timofeev, W. Pfeil, Temperature-induced changes in copper centers and protein conformation of two fungal laccases from *Coriolus hirsutus* and *Coriolus zonatus*, Biochimica et Biophysica Acta 1547 (2001) 397–407.
[27] P. Baldrian, Fungal laccases—occurrence and properties, FEMS Microbiology Reviews 30 (2006) 215–242.
[28] G.I. Makhatadze, P.L. Privalov, Heat capacity of proteins. I. Partial molar heat capacity of individual amino acid residues in aqueous solution: hydration effect, Journal of Molecular Biology 213 (1990) 375–384.
[29] M. Häckel, H.-J. Hinz, G.R. Hedwig, A new set of peptide-based group heat capacities for use in protein stability calculations, Journal of Molecular Biology 291 (1999) 197–213.
[30] S.A. Galema, J.B.F.N. Engberts, H. Høiland, G.M. Førland, Informative thermodynamic properties of the effect of stereochemistry on carbohydrate hydration, Journal of Physical Chemistry 97 (1993) 6885–6889.
[31] J. Gómez, V.J. Hilser, D. Xie, E. Freire, The heat capacity of proteins, Proteins 22 (1995) 404–412.
[32] P.L. Privalov, E.I. Tiktopulo, S.Y. Venyaminov, Y.V. Griko, G.I. Makhatadze, N.N. Khechinashvili, Heat capacity and conformation of proteins in the denatured state, Journal of Molecular Biology 205 (1989) 737–750.
[33] A. Arroyo-Reyna, A. Hernández-Arana, The thermal unfolding of stem bromelain is consistent with an irreversible two-state model, Biochimica et Biophysica Acta 1248 (1995) 123–128.
[34] I.M.C. van Amsterdam, M. Ubbink, M. van den Bosch, F. Rotsaert, J. Sanders-Loehr, G.W. Canters, A new type 2 copper cysteinate azurin, Journal of Biological Chemistry 277 (2002) 44121–44130.
[35] J.W. Donovan, Changes in ultraviolet absorption produced by alteration of protein conformation, Journal of Biological Chemistry 244 (1969) 1961–1967.
[36] J. Wyman Jr., Linked functions and reciprocal effects in hemoglobin: a second look, Advances in Protein Chemistry 19 (1964) 223–286.
[37] W. Pfeil, P.L. Privalov, Thermodynamic investigations of proteins. III. Thermodynamic description of lysozyme, Biophysical Chemistry 4 (1976) 41–50.
[38] Y.V. Griko, Energetic basis of structural stability in the molten globule state: α-lactalbumin, Journal of Molecular Biology 297 (2000) 1259–1268.
[39] Y.V. Griko, P.L. Privalov, Thermodynamic puzzle of apomyoglobin unfolding, Journal of Molecular Biology 235 (1994) 1318–1325.
[40] C. Wang, M. Eufemi, C. Turano, A. Giartosio, Influence of the carbohydrate moiety on the stability of glycoproteins, Biochemistry 35 (1996) 7299–7307.
[41] C.B. Carlson, K.A. Gunderson, D.F. Mosher, Mutations targeting intermodular interfaces or calcium binding destabilize the thrombospondin-2 signature domain, Journal of Biological Chemistry 283 (2008) 27089–27099.
[42] E.I. Shaknovich, A.V. Finkelstein, Theory of cooperative transitions in protein molecules. I. Why denaturation of globular protein is a first-order phase transition, Biopolymers 28 (1989) 1667–1680.
[43] S.J. Hubbard, P. Argos, A functional role for protein cavities in domain:domain motions, Journal of Molecular Biology 261 (1996) 289–300.